A Comparison of Material Measurement Accuracy of RF Spot Probes to a Lens-Based Focused Beam System

John W. Schultz*, James G. Maloney, Kathleen Cummings-Maloney, Rebecca B. Schultz
Compass Technology Group
Roswell, GA USA
john.schultz@compasstech.com

Juan G. Calzada, Bryan C. Foos
Air Force Research Laboratory
Dayton, OH, USA

***Abstract*— A popular method for microwave characterization of materials is the free-space focused beam technique, which uses lenses or shaped reflectors to focus energy onto a confined region of a material specimen. In the 4-18 GHz band, 60 cm diameter lenses are typically spaced 30 to 90 cm from the specimen under test to form a Gaussian beam with plane-wave characteristics at the focal point. This method has proved popular because of its accuracy and flexibility. Another free-space measurement technique employed by some uses dielectrically loaded antennas placed in close proximity to a specimen. In this alternate technique, the dielectrically loaded antennas are smaller than lenses, making the hardware more compact and lower cost, however this is done at the expense of potentially reduced accuracy. This paper directly compares a standard laboratory focused beam system to a measurement system based on recently developed RF spot probes. The spot probes are specially designed antennas encapsulated in a dielectric and optimized to provide a small illumination spot 3 to 8 cm in front of the probe. Several dielectric, magnetic, and resistive specimens were measured by both systems for direct comparison. With these data, uncertainty analysis comparisons were made for both fixtures to establish measurement limits and capability differences between the two methods. Understanding these uncertainties and measurement limits are key to implementing spot probes in a manufacturing setting for quality assurance applications.**

I. INTRODUCTION

Measurement of the dielectric or magnetic properties of materials at microwave frequencies often uses a method where electromagnetic energy is transmitted onto a specimen, and the transmission and/or reflection of energy from that specimen determines the intrinsic permittivity and permeability. A popular implementation of this method is the free-space, focused beam [1,2]. A focused beam device combines feed antennas with focusing elements, which consist of either lenses or shaped reflectors. These focusing elements provide a means for controlling the beam width and phase taper of the energy incident on a material specimen. In particular a focus is formed in front of the lens or reflector, and the specimen is placed at that focus where the phase taper is minimized and the fields can be approximated as plane-wave like.

The focused beam method is popular because of its relative accuracy in characterizing both dielectric and magnetic materials. An example of a typical measurement system is shown in Figure 1. The system pictured in this Figure is a lens-based system and characteristic dimensions are shown to indicate typical size. This system is designed to work at frequencies of 2 GHz and higher and is approximately 300 cm (10 feet) in length. In a laboratory setting, a measurement fixture of this size is usually not a problem, however there are situations in which a more compact measurement method may be needed.

In particular, it is sometimes desirable to conduct measurements of material specimens 'in-situ', where the sensor is small enough to be brought to the component under test. In the hardware shown in Figure 1, the focused beam apparatus is a large, fixed system and a material specimen must be mounted ***in*** the fixture. However in a manufacturing or 'field' setting, the components-under-test may be of the same size or larger than the focused beam fixture. In this case it is necessary to have a measurement sensor that is small enough to be brought to the component-under-test rather than the other way around. This paper discusses just such a sensor, and examines the compromises that are made to realize 'in-situ' measurements that are enabled by a more compact, free-space measurement sensor.

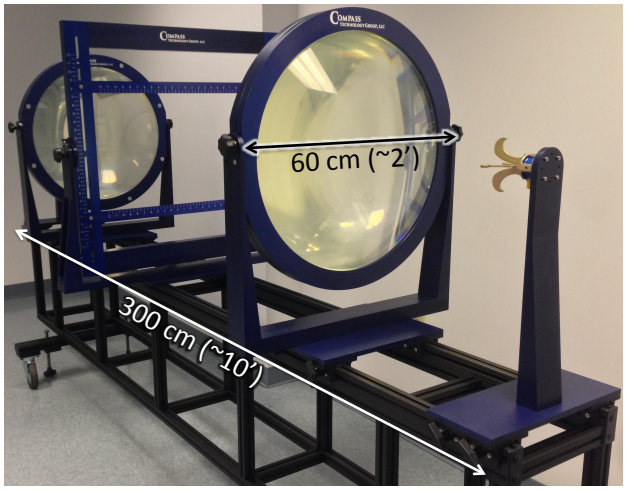

Figure 1. Photograph of a laboratory focused beam system

II. RF Spot Probe Description

The idea of a compact dielectric probe sensor for free space microwave material measurements goes back at least several decades. In the mid 1970s, Musil, Zacek, et al. used dielectric rod antennas to measure transmission through a material specimen [3]. Their sensors consisted of dielectric rods inserted into the ends of horn antennas, which were then placed immediately adjacent to a material specimen. They used their probes to successfully determine the complex dielectric permittivity of Si specimens at millimeter wave frequencies

More recently Diaz et al. used computational simulation tools to design a more sophisticated dielectric rod antenna. This 'polyrod' antenna includes multiple layers inserted into a metal horn antenna [4]. Computational tools were applied to optimize the impedance match of the probe antenna, and their design placed the ends of the dielectric rod a small distance away from the specimen under test, rather than in direct contact.

The spot probe evaluated in the present work also includes both metallic elements and dielectric material. However while previous spot probes designed dielectric rods into conventional horn antennas, the present probe design optimizes both the dielectric shape and metallic elements into an integrated unit. The result is a very compact and rugged design that has excellent wide band performance. Figure 2 is a photograph of these integrated spot probes and shows their compact shape. The probes are fed with a single SMA port in the rear, and they transmit and receive with linear polarization from 2.5 to 20 GHz. These probes are 18 cm (7 inches) long and 5.1 cm (2 inches) in diameter.

Figure 2. Photograph of RF spot probes

The spot probe design was iteratively optimized with a Finite Difference Time Domain (FDTD) code named OpenTDA, which can also be used to evaluate the local fields radiated by the probe. The simulations launched a wide-band pulse from a coaxial port and marched through time to determine the E and H fields within the simulation space. Frequency domain plots can then be calculated with a Fourier transform of the time-domain signals. An example plot of the E-fields emanating from the tip of the probe at 9 GHz are shown in Figure 3. The x- and y- axes are position coordinates centered at the tip of the probe, and the field strength is shown in dB. The plotted data is normalized to the peak field at the probe tip. There are two white lines overlaid on the plot that indicate the 3-dB width of the radiating beam at each x-axis position. As these lines indicate, the 'focus' of the beam is at the probe tip and the beam diameter therefore grows with distance from the probe tip. At 2.5 cm (1 inch) from the probe tip the beam diameter is approximately 3 cm (1.2 inches). At 7.6 cm (3 inches) from the probe tip, the beam diameter is approximately 6.3 cm (2.5 inches) The data in Figure 3 are for an H-field plane cut and a similar beam shape can be seen in the E-plane.

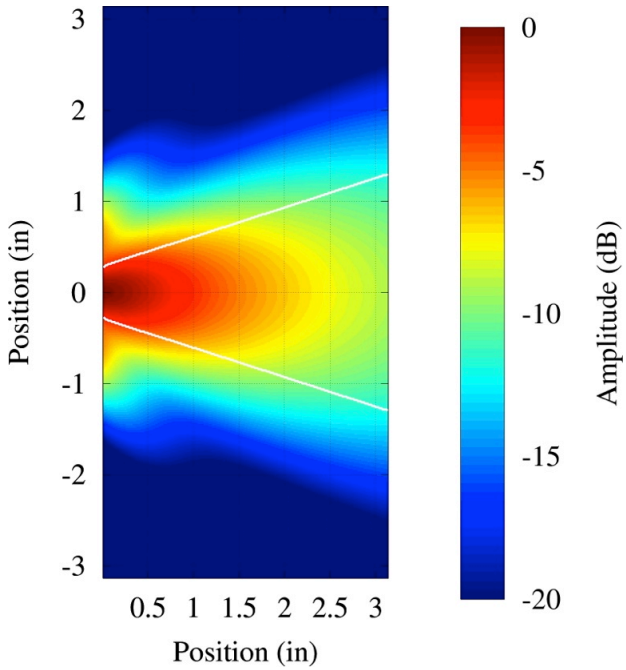

Figure 3. Computed E-fields at end of probe at 9 GHz

In the plots that follow, a 7 cm (2.75 inch) standoff distance between the probe tip and the specimen under test is used. Other standoff distances may be used depending on the measurement geometry constraints. When a pair of probes is used for both reflection and transmission measurements, the probe separation is therefore 14 cm (5.5 inches). Having some separation between the probe and the material under test provides a safety margin in situations where the test article may be damaged by direct contact. It also enables room for insulation layers if high-temperature measurements are required.

Figure 4 shows the E-plane and H-plane beam width, 7 cm in front of the tip for a series of different frequencies. Because the probe has a fixed physical aperture, the beam width decreases with frequency. The data show that the average beam width of the probe at this standoff distance varies between 4 and 11 cm within its operating bandwidth, and that the beam profile is approximately (though not exactly) circular in shape. Finally, the measured S11 amplitude from one of the probes is shown in Figure 5. These data show that the probe operates from approximately 2.5 GHz to 20 GHz.

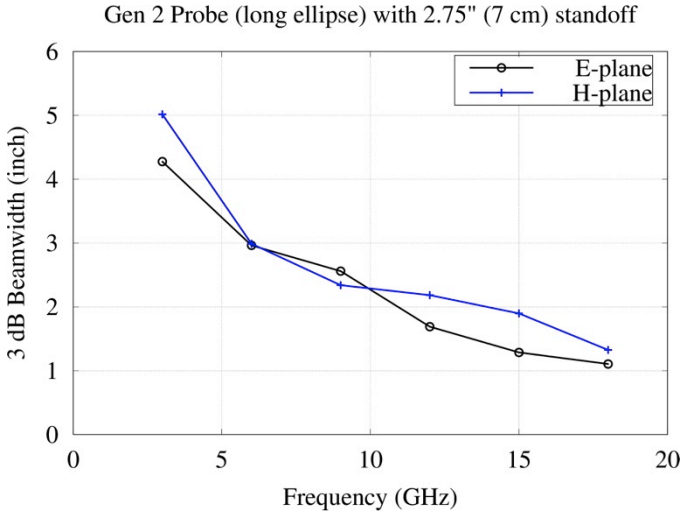

Figure 4. Calculated E- and H-plane beam width 7 cm (2.75 inches) from end of probe

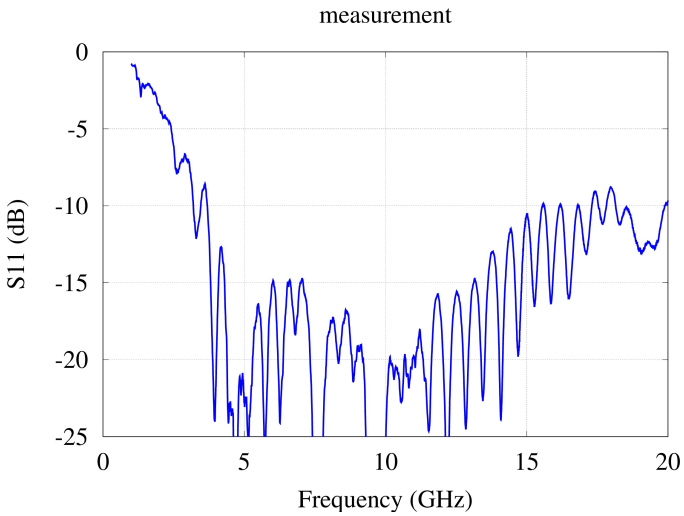

Figure 5. Measured VSWR of probe showing wideband performance

III. Measurment Uncertainties

Comparing measurements made by the spot probes to a laboratory focused beam fixture begins by noting that the obvious hardware differences. The large diameter lens is able to project a focus some distance in front, while a small probe does not have sufficient aperture area to do the same. This is important because the phase taper across a beam is minimized at the focus. Thus while the focused beam fixture gives an excellent approximation to a single plane wave, the spot probe will always have some phase taper. Note that the focused beam apparatus used for this effort was based on a common lens shape employed by many laboratories and originally developed at Georgia Tech [5]. The lenses are fed by 2 to 32 GHz, open-boundary, quad-ridge antennas manufactured by Satimo [6].

The small aperture of the RF spot probe also results in a reduced received signal level when compared to a focused beam system. Figure 6 shows the insertion loss measured from both a focused beam and a pair of spot probes. The cables were included in the calibration so that the plotted insertion loss only includes effects from the fixture (i.e. from the feed horns and lenses for the focused beam and the probes for the probe system) and not attenuation through the cables. Both fixtures have mismatch reflections for each of their components, so some of the insertion loss experienced by both is due to these mismatches. Additionally the probe fixture shows 5 to 10 dB more insertion loss compared to the focused beam. This increase is due to additional space loss caused by incomplete capture of the energy emitted by the transmit probe. With this small increase in insertion loss, we can assume that the measurement noise floor for the probe should only be a little higher than that of the focused beam system, all else being equal.

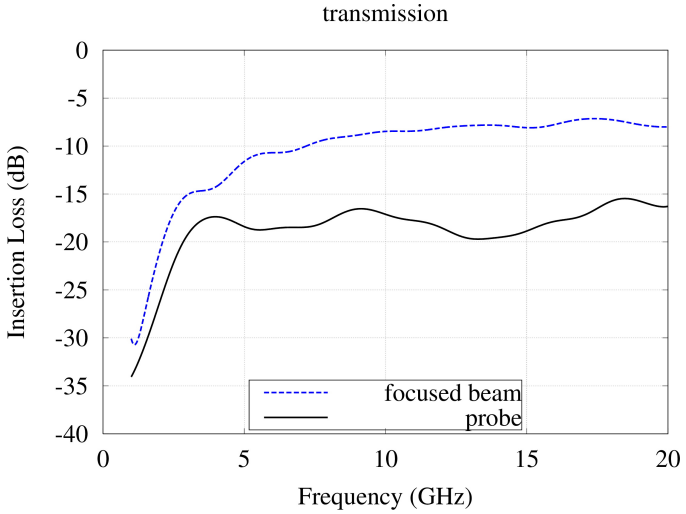

Figure 6. Measured insertion loss of both measurement fixtures with no specimen (not including cables)

Another potential difference between measurements with the spot probes and the focused beam is calibration. In the measurement data shown in this paper, a “response and isolation” method was used for both measurement systems. The response standard for transmission is a thru and the response standard for reflection is a flat metal plate, and both measurement fixtures used these standards. Additionally, specimen-positioning errors were minimized by measuring

four S-parameters (S11, S22, S21 and S12) using the procedure described in [2]. However, the isolation standards for S11 and S22 differed for the two fixtures. For the focused beam a metal plate tilted 45 degrees was used as an isolation standard. The isolation standard directed the energy away from the measurement system and is equivalent to a matched load, which helps to account for reflections from the lens, feed horn, and network analyzer ports. For the spot probes, their separation was only 14 cm (5.5 inches) so it was impractical to use this method of isolation standard. Therefore a simplified isolation standard of just free space is used to simulate the matched load. Without the tilted metal plate, this version of the isolation measurement can therefore include undesired reflections from the receive probe, which is in the transmission path just a few inches beyond the specimen position.

Both the beam spreading (space loss) effect and the simplified calibration can impact the measurement noise floor of the probe when compared to the focused beam system. Figure 7 shows a series of calibrated transmission (S21) measurements through a 6.35 mm thick metal plate. Each of these data sets were taken over a time period of at least two to four hours and so they include temperature and instrument drift. Since the metal plate should not transmit microwave energy, the measured signal levels are caused by either leakage within the network analyzer, or energy spilling around the metal plate to the other side of the fixture. To reduce multipath reflections, time domain processing was applied, which converts the frequency data to time domain via a Fourier transform, and puts a 0.5 nanosecond window around the desired signal (to gate out the other noise signals). The same time domain gate was used for both the focused beam and probe data. Thus these data give an indication of the measurement noise floor for a 30 or 60 cm wide specimen.

Comparing the insertion loss of a square 30 cm wide metal plate versus a larger 60 x 60 cm wide plate shows a 30 dB decrease in the noise floor. Thus the primary contribution to the S21 noise floor with a 30 cm specimen is energy that goes around or diffracts off the outer edges. The multiple lines that are plotted do not overlay because the metal plate was removed and replaced between each measurement and so was not placed in exactly the same position each time. Except for the highest frequencies, the focused beam and the probes have comparable insertion loss levels for the 60 cm wide plate.

A rule of thumb for estimating sensitivity limits is that the signal level should be no less than 15 dB above the noise floor. Based on the data of Figure 7, both the laboratory focused beam system and the probes can accurately measure insertion losses as low as -75 dB for specimens that are 60 cm x 60 cm. However when the specimen size is reduced to 30 cm x 30 cm, energy can go around the specimen and accurate measurements can be obtained only down to levels of approximately -30 to -40 dB, depending on frequency. Note that all these estimates apply when a 0.5 ns time-domain gate is applied. If a material is resonant and requires a longer duration gate, then there may be more 'spill-over' energy received, and the 'noise floor' may increase.

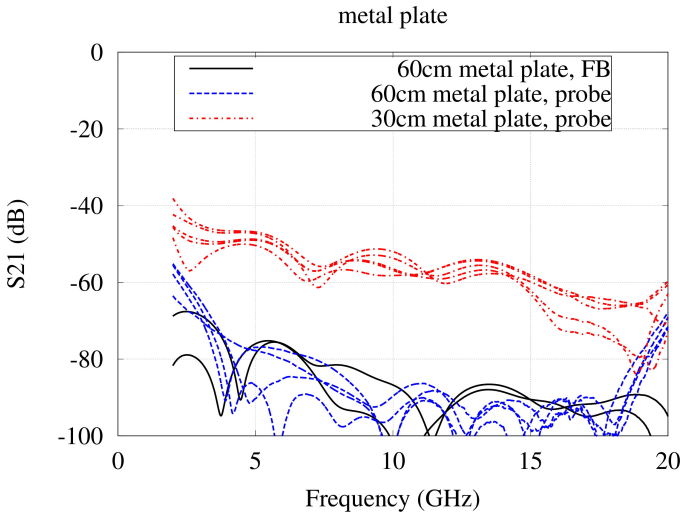

Figure 7. Measured insertion loss of a metal plate showing measurement noise floor

A similar measurement can be made for the reflection noise floor and is shown in Figure 8. Like the transmission data, these reflection data include a time-domain gate of 0.5 nanoseconds. One significant difference between transmission and reflection data is that reflection data is more sensitive to temperature shifts. Because of the finite thermal expansion coefficient of microwave cables, the phase the signal can change even with small (less than a couple degree) changes in the ambient temperature, such as the typical cycling of an air conditioner. In the measurements in Figure 8, the cables were 4 meters long, and a lower noise floor may be obtained by reducing the cable length. As before, the measurements were taken over a 2-4 hour time period. Similar to the transmission measurements, the data indicate that the probes have a reflection noise floor in the same range as the focused beam. Based on the data in Figure 8, reflection measurements should be accurate at least down to levels of -30 to -40 dB.

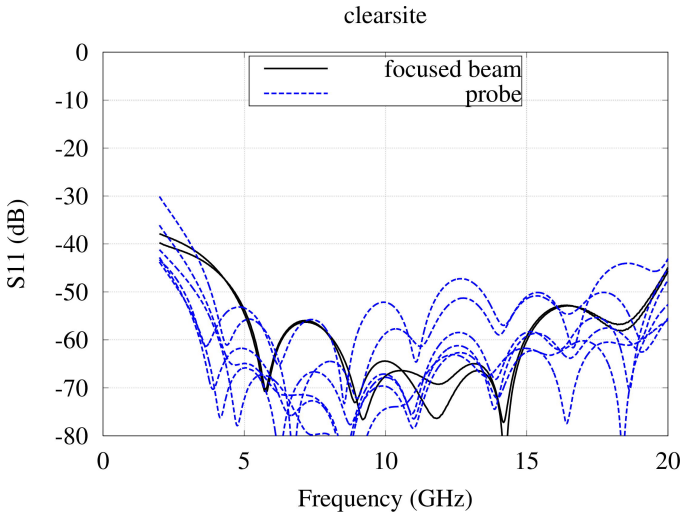

Figure 8 - Measured reflection of a clearsite showing measurement noise floor

While the above results provide some measurement limits of both the laboratory focused beam and RF spot probes, there are additional uncertainties that can occur, particularly in the evaluation of complex properties of materials. The above measurements specifically address amplitude limits, but materials also require phase measurements to fully determine their properties. Determining phase limits is more difficult than amplitude, and is beyond the scope of the present study. However the next section provides some indication of phase accuracy by directly comparing material measurements that include both amplitude and phase.

IV. Comparison Measurements

The focused beam free space technique has become a standard used by many laboratories for determining the permittivity and permeability of materials at microwave frequencies. For this paper, it provides a useful benchmark by which we can judge the accuracy of the spot probes. The most direct way to compare is with measurements of actual materials. Figure 9 shows the measurements of a low-loss slab of acrylic (polymethyl methacrylate). This is a simple dielectric material and the permittivity is determined from the amplitude and phase of the transmission coefficient (S21). In this case a standard iterative method was used to solve for the complex permittivity [2]. Both the real and imaginary permittivity are plotted as a function of frequency in Figure 9, and they show good agreement between the focused beam (FB) and the probe devices.

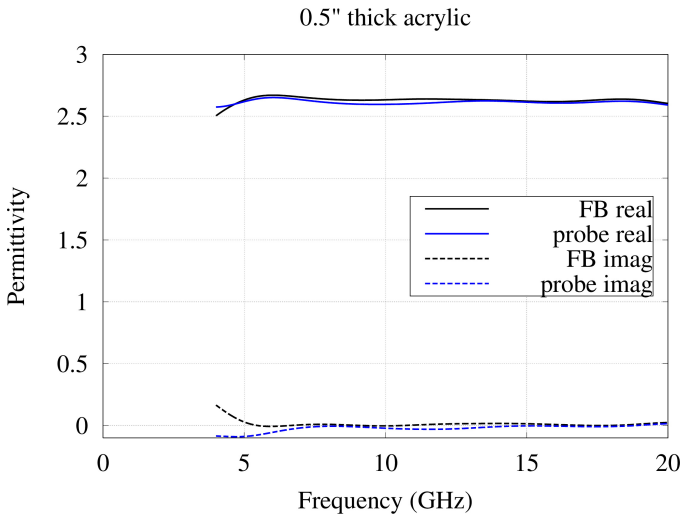

Figure 9. Measured dielectric permittivity of acrylic, solid lines are real permittivity and dotted lines are imaginary

The difference between the real permittivity from the focused beam and the spot probe measurements is no greater than 2.5% at any one frequency. The mean permittivity averaged over the 4-20 GHz band differs by approximately 1% between the two methods. Because the specimen was 30 x 30 cm, the accuracy of both methods degrades below 4 GHz, so only data from 4 GHz and up are shown.

A more challenging material to measure is one that has both magnetic and dielectric properties, and Figure 10 shows measurements of a commercial magnetic absorber. This particular material is a polyurethane filled with iron powder. The dielectric permittivity is shown in the top plot while the bottom plot shows the magnetic permeability. The real permittivity or permeability are shown as solid lines while the imaginary data are shown as dotted lines. These data were inverted from both transmission and reflection and all four scattering parameters (S11, S22, S21, S12) were used. The four-parameter method enables the specimen position to be determined without need for a physical measurement. This method minimizes reflection phase errors that occur from displacement of the specimen relative to the calibration plane [2] (i.e. which happens with a flexible material).

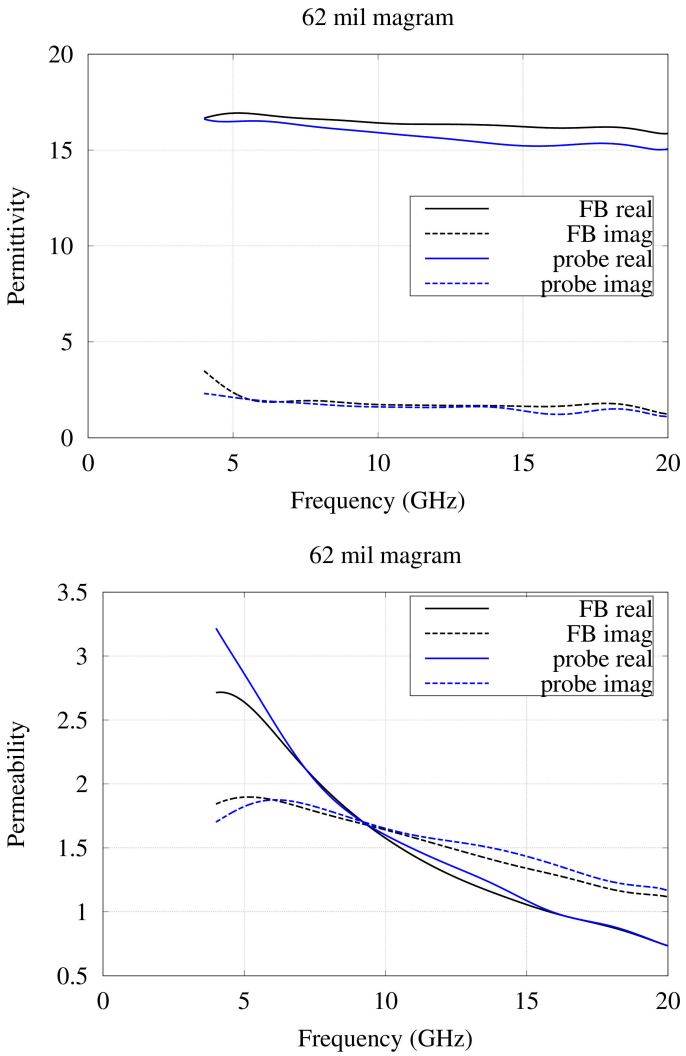

Figure 10. Measured dielectric permittivity (top) and magnetic permeability (bottom) of a commercial magnetic absorber

As the data in Figure 10 show, the probe agrees well with the focused beam even in a full two-port measurement where

amplitude and phase of all the S-parameters are used. In this case the difference between the focused beam and the probe is no worse than 7% for most of the measured frequencies. A band-averaged comparison cannot be made because of the dispersive nature of this material. Like the acrylic, this magnetic specimen was only 30 x 30 cm in size, so accuracy degrades at the lowest frequencies.

The final class of materials tested was a series of commercially available resistive sheets (R-cards). These materials consisted of thin alloy layers on 3 to 6 mil (75 to 150 micron) Mylar substrates. The comparison between the focused beam and the probes is shown in Figure 11, which shows measured data from 6 different specimens. Plotted are the real impedances of these sheets, ranging over several orders of magnitude from 4 ohms/square to 1000 ohms/sq. The agreement between the focused beam (FB) and the probe data is good, and the band-averaged impedances agree within two percent for all except the 1200 ohm/square specimen. Note that the lowest impedance specimen, 4 ohms/square corresponds to an insertion loss of -34 dB while the highest impedance specimen, 1100 ohms/square corresponds to an insertion loss of approximately -1.4 dB.

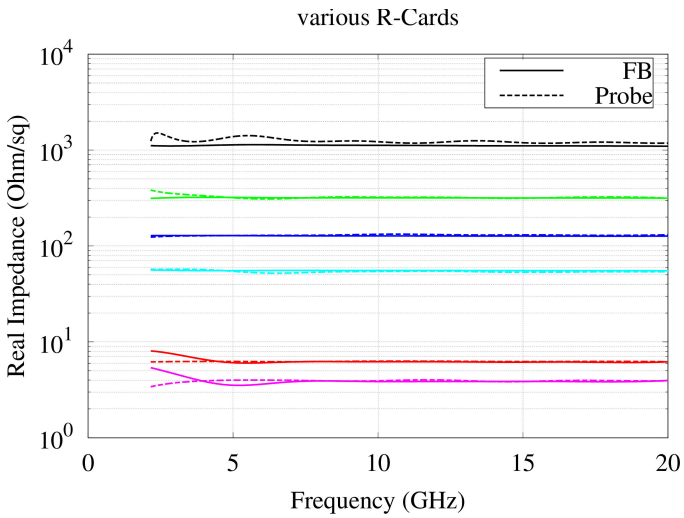

Figure 11. Measured sheet impedance of commercially available resistive sheets.

V. Conclusions

This paper compares microwave material measurements made by two different free space fixtures: a lens-based focused beam and compact spot probes. The spot probes, which are specially designed dielectric antennas, do not generate a focused spot as well as a lens system. In particular, the phase taper in front of the probe is not as flat as what can be obtained with dielectric lenses or shaped reflectors. However even with this limitation, the spot probes still have excellent measurement accuracy for a wide variety of material specimens at normal incidence.

In this paper, the two measurement methods were evaluated against low-loss dielectric, magnetic radar absorbing material, and resistive sheets. Measurements were made from 2 to 20 GHz and material properties were calculated from the S-parameter data. With material inversions that use only transmission (S21) measurements, the probes provided measured material parameters that agreed with a focused beam system to within a couple of percent. When the material measurements included both transmission and reflection, the agreement was not quite as exact, but the dielectric and magnetic properties determined with spot probes still matched the focused beam data to better than 7% over most of the frequencies measured.

Acknowledgements

The authors would like to thank Mr. Kurt Weissmayer and Mr. Jeremy Wooten of Weissmann Tool for their expertise in constructing the RF spot probes.

References

[1] J. Musil, F. Zacek, Microwave Measurement of Complex Permittivity by Free Space Methods and their Applications, Elsevier, New York, 1986

[2] J.W. Schultz, Focused Beam Methods: Measuring Microwave Materials in Free Space, CreateSpace Publishing, 2012

[3] J. Musil, F. Zacek, A. Burger, J. Karlovsky, "New Microwave System to Determine the Complex Permittivity of Small Dielectric and Semiconducting Samples," 4th European Microwave Conference, 66-70, 1974

[4] R. Diaz, J. Peebles, R. Lebaron, Z. Zhang, L. Lozano-Plata, "Compact Broad-Band Admittance Tunnel Incorporating Gaussian Beam Antennas," U.S Patent 788948, 2007

[5] D.R. Reid, G.S. Smith, "A Comparison of the Focusing Properties of a Fresnel Zone Plate With a Doubly-Hyperbolic Lens for Application in a Free-Space, Focused-Beam Measurement System," IEEE trans AP, 57(2), 499-507, 2009

[6] Satimo Corporation, datasheet for "Open Boundary Wideband Quad Ridge Horns," Model QH 2000, www.satimo.com, 2013